

See discussions, stats, and author profiles for this publication at: <https://www.researchgate.net/publication/231667498>

Giant Enhancement of the Second Hyperpolarizabilities of Open-Shell Singlet Polyaromatic Diphenalenyl Diradicaloids by an External Electric Field and Donor-Acceptor Substitution

ARTICLE *in* JOURNAL OF PHYSICAL CHEMISTRY LETTERS · APRIL 2011

Impact Factor: 7.46 · DOI: 10.1021/jz200383a

CITATIONS

47

READS

47

11 AUTHORS, INCLUDING:



Masayoshi Nakano

Osaka University

334 PUBLICATIONS 4,714 CITATIONS

SEE PROFILE



Shabbir Muhammad

King Khalid University

58 PUBLICATIONS 583 CITATIONS

SEE PROFILE



Ryohei Kishi

Osaka University

110 PUBLICATIONS 1,930 CITATIONS

SEE PROFILE



Yasuteru Shigeta

University of Tsukuba

174 PUBLICATIONS 1,804 CITATIONS

SEE PROFILE

Giant Enhancement of the Second Hyperpolarizabilities of Open-Shell Singlet Polyaromatic Diphenalenyl Diradicaloids by an External Electric Field and Donor–Acceptor Substitution

Masayoshi Nakano,^{*,†} Takuya Minami,[†] Kyohei Yoneda,[†] Shabbir Muhammad,[†] Ryohei Kishi,[†] Yasuteru Shigeta,[†] Takashi Kubo,[§] Léa Rougier,^{||} Benoît Champagne,^{||} Kenji Kamada,[‡] and Koji Ohta[‡]

[†]Department of Materials Engineering Science, Graduate School of Engineering Science, Osaka University, Toyonaka, Osaka 560-8531, Japan

[§]Department of Chemistry, Graduate School of Science, Osaka University, Toyonaka, Osaka 560-0043, Japan

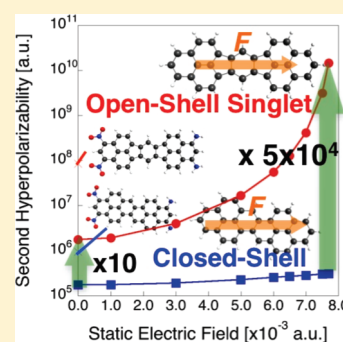
^{||}Laboratoire de Chimie Théorique (LCT), Facultés Universitaires Notre-Dame de la Paix (FUNDP), Rue de Bruxelles 61, B-5000 Namur, Belgium

[‡]Research Institute for Ubiquitous Energy Devices, National Institute of Advanced Industrial Science and Technology (AIST), Ikeda, Osaka 563-8577, Japan

S Supporting Information

ABSTRACT: Switching on an external electric field (F) along the electron correlation direction produces a giant enhancement of the second hyperpolarizability γ in a polyaromatic diradicaloid having intermediate diradical character. This has been evidenced by carrying out spin-unrestricted density functional theory calculations with the LC-UBLYP long-range corrected exchange-correlation functional for the *s*-indaceno[1,2,3-*cd*;5,6,7-*c'd'*]diphenylene (IDPL) diradical compound in comparison to a closed-shell analogue of similar size composed of two pyrene moieties (PY2). For IDPL, the field-induced enhancement ratio is estimated to reach 4 orders of magnitude for an electric field of 0.0077 a.u., whereas it is less than a factor of 2 for PY2. Moreover, an enhancement is also observed by substituting both-end phenalenyl rings of IDPL with donor (NH_2)/acceptor (NO_2) groups, but this enhancement is limited to about 2 orders of magnitude. These enhancements are associated with a reduction of the diradical character (and therefore an improved thermal stability) as well as with the appearance of substantial type-I contributions to γ .

SECTION: Molecular Structure, Quantum Chemistry, General Theory



One of the recent hot topics lies in the exploration of the intriguing electronic and spin functionalities of polyaromatic hydrocarbons (PAHs) including graphenes^{1,2} as well as in the establishment of rational design guidelines toward achieving targeted functionalities.^{3–6} In particular, in their open-shell singlet ground states, these PAHs have attracted a great deal of attention not only from theoreticians but also from experimentalists with the view of extending the concept of “chemical bond” — by realizing flexible chemical bonds associated with intermediate and strong electron correlations^{7–12}— and of developing a novel class of functional materials for applications in electronics, photonics, and spintronics.^{13–17} Because the electronic structures of such unique open-shell singlet ground states are characterized by the “diradical character”,^{18–23} unraveling the relationships between their properties and the diradical character is a key issue. Therefore, this has been achieved for physical quantities associated with electronic excitations (excitation energies, transition moments, and dipole moments) by considering a general two-site model using the valence configuration interaction

(VCI) scheme.²⁴ On the basis of this analysis, we have presented a novel structure–property relationship between the second hyperpolarizability (γ) and the diradical character; open-shell singlet molecules exhibit significant γ enhancement in the intermediate diradical character region as compared to closed-shell and pure open-shell systems with similar conjugation lengths.^{24,25} This relationship has been exemplified by using ab initio molecular orbital (MO) and density functional theory (DFT) calculations for several open-shell singlet systems including aromatic compounds including imidazole rings,²⁶ diphenalenyl diradicaloids,²⁷ transition-metal-involving systems,²⁸ and nanographenes.²⁹ The success in the synthesis of stable PAHs involving diphenalenyl rings^{8,11} has enabled the measurements of their two-photon absorption (TPA) properties (which are typical third-order nonlinear optical effects and, at the molecular level, are described by γ).

Received: March 22, 2011

Accepted: April 15, 2011

Published: April 19, 2011

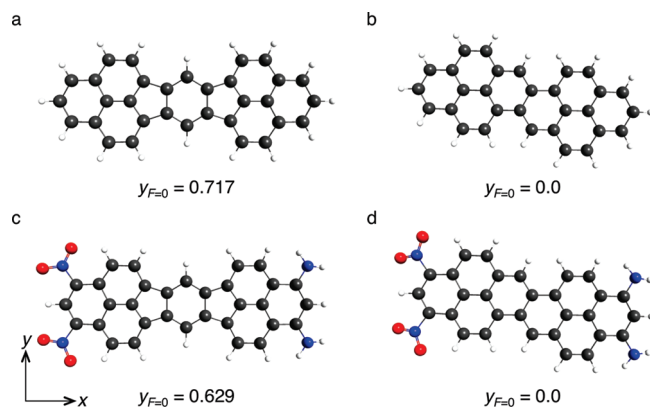


Figure 1. Molecular structures (gray: carbon; blue: nitrogen; red: oxygen; white: hydrogen) of IDPL (a), PY2 (b), DA-IDPL [(NO₂)₂-IDPL-(NH₂)₂] (c), and DA-PY2 [(NO₂)₂-PY2-(NH₂)₂] (d) (in the absence of an electric field) optimized by the (U)B3LYP/6-31G* method. The middle carbon–carbon bonds of PY2 and DA-PY2 form an angle of 60° with the longitudinal (*x*) axis. The diradical characters ($y_{F=0}$) in the absence of a field calculated by the LC-UBLYP/6-31G* method are also shown.

Thus, the theoretical predictions have been confirmed by the experimental observation of the remarkable TPA cross sections in the open-shell singlet *s*-indaceno[1,2,3-*cd*;5,6,7-*c'd'*]diphenylene (IDPL) compound displaying intermediate diradical character.³⁰

Extending the VCI scheme, a further enhancement and control scheme of γ in these open-shell singlet systems was subsequently proposed by considering the application of a static *pump* electric field. Indeed, it results in a gigantic enhancement of γ (~ 2 – 3 orders) in symmetric diradicals having intermediate diradical characters with respect to those of closed-shell and pure diradical molecules in the absence of a pump field.³¹ However, because this prediction has not yet been confirmed, except for simple model diradical systems such as the H₂ molecule under dissociation and the twisted ethylene,³¹ we investigate, in this Letter, the effects of applying a pump electric field on γ of realistic PAH systems, that is, IDPL as well as a similar-size closed-shell analogue composed of two pyrene moieties (PY2). In addition, the donor (NH₂)–acceptor (NO₂) substitution effects on the γ of these systems are examined because they cause asymmetric electronic distributions similar to those observed in systems under a static field.^{32,33}

Figure 1 displays the structures of IDPL (a) and PY2 (b) as well as of their donor (NH₂)/acceptor (NO₂) substituted counterparts, DA-IDPL (c) and DA-PY2 (d), in their singlet ground states in the absence of an electric field, which were optimized by the (U)B3LYP/6-31G* method. The optimized structures of IDPL and PY2 are planar (in the *x*–*y* plane) with *D*_{2h} and *C*_{2h} symmetries, respectively, while those of the donor–acceptor substituted counterparts are planar, except for the slightly out-of-plane substituent groups (see Tables 1S–6S and Figure 1S in Supporting Information). The amplitude of the static pump electric field ranges from 0.0 to 0.0077 a.u. (0.0 to 0.4 V/Å), that is, similar to those used for “half-metallicity” of graphenes.¹⁴ The field is applied along the longitudinal (*x*) direction, and the field-dependent geometries are optimized in the *x*–*y* plane (see Tables 1S–6S and Figure 1S in Supporting Information).³⁴ In this Letter, the occupation number (n_{LUNO}) of the lowest unoccupied natural orbital (LUNO) calculated using the LC-UBLYP/6-31G* method is employed to estimate

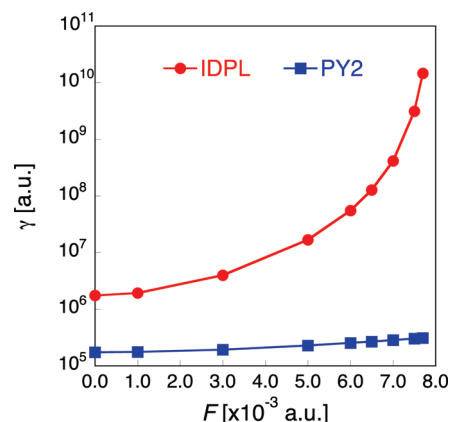


Figure 2. Static electric field ($F = 0.0$ – 0.0077 a.u.) effect on γ_{xxxx} [a.u.] of IDPL and PY2 calculated by the LC-UBLYP/6-31G* method.

the diradical character y_F . y_F takes a value ranging from 0 (closed-shell) to 1 (pure diradical). Although the diradical character was originally defined within the multiconfigurational self-consistent field (MC-SCF) theory as twice the weight of the doubly excited configuration in the singlet ground state,^{18,19} the fractional occupation number of the LUNO in spin-unrestricted (U) single determinant schemes (like UDFT) is alternatively employed because these values reproduce the former ones well. The definitions and physical meaning of the diradical character have been discussed in several papers in connection with the odd electron number and density,^{20–22} which are not observable but provide an index of the chemical bond.

The dominant longitudinal electronic γ values (γ_{xxxx}) of these systems are calculated using the LC-UBLYP/6-31G* method with a range separating parameter of $\mu = 0.33$ ³⁵ by adopting the finite-field approach, which consists in the fourth-order differentiation of the energy with respect to the *probe* electric field (F') while the system undergoes the effects of the *pump* field (F)³⁶

$$\gamma(F) = \lim_{F' \rightarrow 0} \frac{1}{36F'^4} [E(F + 3F') - 12E(F + 2F') + 39E(F + F') - 56E(F) + 39E(F - F') - 12E(F - 2F') + E(F - 3F')] \quad (1)$$

The LC-UBLYP method has been found to semiquantitatively reproduce the γ of several open-shell molecules calculated with the highly correlated spin-unrestricted coupled cluster method including single and double excitations with a perturbative treatment of the triple excitations.³⁷ The spatial contributions to γ are unraveled using the γ density analysis,³⁸ which utilizes the plots of the third-order derivative of the electron density with respect to the electric field; the positive and negative γ densities represent the field-induced increase and decrease in the third-order electron density, respectively. All calculations were performed using the Gaussian 09 program package.³⁹

IDPL and PY2 are regarded as singlet open-shell and closed-shell systems, respectively, as seen from their diradical characters, $y_{F=0} = 0.717$ (IDPL) versus 0.0 (PY2). Such diradical character in IDPL is exemplified by the dominant spin polarization on the both-end phenalenyl rings (see Figure 2S in Supporting Information). The donor–acceptor substitution of these rings reduces $y_{F=0}$ from 0.717 (IDPL) to 0.629 (DA-IDPL). The same trend is observed in IDPL when applying an external electric field. For instance, the y_F amplitude goes down to 0.293 at

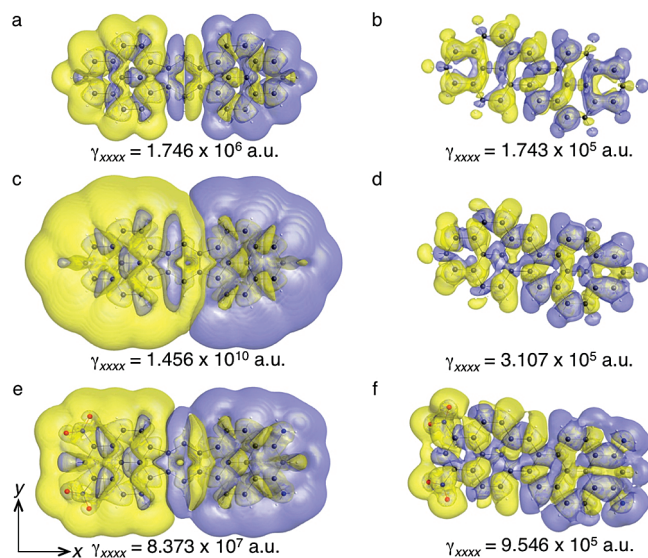


Figure 3. γ_{xxxx} density distributions and γ_{xxxx} values of IDPL (a,c) and PY2 (b,d) at $F = 0.0$ and 0.0077 a.u. as well as of DA-IDPL (e) and DA-PY2 (f) calculated by the LC-UBLYP/6-31G* method. The yellow and blue meshes represent positive and negative densities, respectively, with isosurfaces of ± 100 a.u.

$F = 0.0077$ a.u. (see Table 7S in Supporting Information). Such field effects on γ_F are predicted to be caused by the field-induced increase of the weight of the ionic component in the ground state, the mechanism of which has been explained in our previous study.³¹ Indeed, at $F = 0.0077$ a.u., the amount of charge transfer (CT) from the right- to the left-hand side (obtained from the Mulliken net charges shown in Figure 3S in Supporting Information) of IDPL is 0.427 [the x component of the ground-state dipole moment ($\mu_{gx} = 9.88$ a.u.)], which is significantly larger than that in the pyrene rings (0.270) of PY2 ($\mu_{gx} = 5.76$ a.u.), while the IDPL spin densities are reduced and asymmetrized (see Figure 2S in Supporting Information). Figure 2 displays the evolution of γ of IDPL and PY2 for the fields ranging from 0.0 to 0.0077 a.u.. It is found that (i) the γ values of both systems increase with F , that is, $\gamma = 1.746 \times 10^6$ (IDPL) versus 1.743×10^5 a.u. (PY2) at $F = 0.0$ a.u. and $\gamma = 1.456 \times 10^{10}$ (IDPL) versus 3.107×10^5 a.u. (PY2) at $F = 0.0077$ a.u.; (ii) γ is larger in IDPL than that in PY2 in the whole F region; and (iii) the enhancement ratio, $\gamma(\text{IDPL})/\gamma(\text{PY2})$, also increases with F , that is, $\gamma(\text{IDPL})/\gamma(\text{PY2}) = 10$ ($F = 0.0$ a.u.) versus 4.7×10^4 ($F = 0.0077$ a.u.). Such a giant field-induced increase of γ in IDPL relative to that in PY2 is substantiated by the remarkable enhancement of the γ density amplitudes (see Figure 3a–d). When $F = 0$, the extended positive and negative π electron γ densities (distributed on the left- and right-hand phenalenyls, respectively) provide the dominant positive contribution to γ of IDPL (Figure 3a), while for PY2 (Figure 3b), the γ density amplitudes are smaller, and both positive and negative γ densities alternate in the middle region, which significantly cancels the positive contribution to γ . Applying an electric field in the x -direction causes a significant enhancement of the γ density amplitudes, in particular, in IDPL, with slightly asymmetric γ density distributions in the x -direction. This enhances the differences between IDPL (Figure 3c) and PY2 (Figure 3d), though the distribution topologies are the same as those in the $F = 0$ case (Figure 3a and b). The sites with dominant γ density distributions on the phenalenyl moieties of IDPL coincide

with those having the major spin densities (see Figure 2S in Supporting Information), which confirms that the spin-polarized π -electrons between the left- and the right-hand phenalenyl rings contribute to the γ enhancement in IDPL. Moreover, within the two-site VCI model,³¹ the field-dependent γ values are given by a three-state formula (the three contributing singlet states are the ground (g), the first (k), and the second (f) excited states), but the remarkable field-induced enhancement of γ of IDPL is predicted to originate from the two-state type-I virtual excitation processes

$$\gamma^I = 4 \frac{(\mu_{kg})^2 (\Delta\mu_{kk})^2}{(E_{kg})^3} \quad (2)$$

which involve the excitation energy (E_{kg}), the transition moment (μ_{kg}), and the dipole moment difference ($\Delta\mu_{kk}$) between the ground and the second excited states.^{31,37} This suggests that the pump field induces in IDPL (intermediate diradical system) a larger decrease of E_{kg} and larger increases of $|\mu_{kg}|$ and $|\Delta\mu_{kk}|$ than those in PY2 (closed-shell system).

The lowest-order contributions to the vibrational γ were also calculated for IDPL and PY2 (in the limit of no external pump field) by using the finite-field nuclear relaxation approach,⁴⁰ which is based on calculating lower-order molecular properties (here, α and β) by considering both the electronic and nuclear field-induced relaxations. The nuclear relaxation contributions to electric field-induced second harmonic generation [$\gamma(-2\omega; \omega, \omega, 0)$] and the dc-Kerr effect [$\gamma(-\omega; \omega, 0, 0)$] were calculated in the infinite optical frequency limit at the LC-UBLYP level. They amount to 0.06×10^6 and 0.18×10^6 a.u. for IDPL, whereas they are less than 0.01×10^5 and 0.80×10^5 a.u. for PY2, respectively. Thus, the vibrational counterparts attain 3–10 and 0–46% of the static electronic γ values for IDPL and PY2, respectively.

On the other hand, instead of applying a static electric field, we can achieve a similar situation by using donor (NH_2)–acceptor (NO_2) substitution into PAHs, that is, DA-IDPL [$(\text{NO}_2)_2$ -IDPL- $(\text{NH}_2)_2$] and DA-PY2 [$(\text{NO}_2)_2$ -PY2- $(\text{NH}_2)_2$] (Figure 1c and d). Indeed, DA-IDPL and DA-PY2 exhibit CTs from the right- to the left-hand side qualitatively similar to those of IDPL and PY2 under the applied fields, though the amounts of CT of DA-IDPL (0.162) and DA-PY2 (0.153) are smaller than those [0.427 (IDPL) and 0.270 (PY2)] at $F = 0.0077$ a.u. (see Figure 3S in Supporting Information). From comparing the γ values of DA-IDPL and IDPL with the field (see Tables 7S and 8S in Supporting Information), the two donor–acceptor pairs cause an effect on γ comparable to a field of approximately 0.0060 – 0.0065 a.u.. Indeed, γ of DA-IDPL amounts to 8.373×10^7 a.u., in comparison to $\gamma = 5.501 \times 10^7$ – 1.278×10^8 a.u. with $F = 0.0060$ – 0.0065 a.u.. On the other hand, electric field amplitudes of 0.0077 a.u. or smaller are not enough to reproduce the γ value of DA-PY2 (9.546×10^5 a.u.), substantiating the fact that the relationship between D/A pairs and that external electric field is not universal and depends on the nature of the linker,³³ in other words, in this case, from the orbital interactions between the donor–acceptor groups and IDPL/PY2 moieties. Nevertheless, the γ value of DA-IDPL (8.373×10^7 a.u.) is about 88 times larger than that of DA-PY2 (9.546×10^5 a.u.), the ratio of which is strongly enhanced relative to the unsubstituted case at $F = 0$, $\gamma(\text{IDPL})/\gamma(\text{PY2}) = 10$. This enhancement is further exemplified by the γ density distributions shown in Figure 3e and f. The dominant positive contribution to γ in DA-IDPL originates from the virtual CT between both-end substituted phenalenyl rings, the feature of which is similar to the field effect (see Figure 3a and e). Similarly to PY2 under a static field, positive and negative

γ densities appear alternately in the middle regions of DA-PY2, which significantly cancel the positive contribution to γ (see Figure 3d and f).

In summary, switching on an electric field (F) along the electron correlation direction produces a giant enhancement of γ in the polyaromatic diradicaloid having intermediate diradical character. Therefore, for IDPL, the enhancement with respect to the field-free case is 4 orders of magnitude when switching on an electric field of 0.0077 a.u.. This contrasts with the weak field effect observed in similar-size closed-shell analogues like PY2, which also corroborates previous investigations showing that the γ enhancement in closed-shell π -conjugated systems is typically 1 order of magnitude.^{32,33} Moreover, this γ enhancement ratio between open-shell and closed-shell compounds gets larger with the field amplitude, $\gamma(\text{IDPL})/\gamma(\text{PY2}) = 10$ ($F = 0.0$ a.u.) versus 4.7×10^4 ($F = 0.0077$ a.u.), while similar effects are achieved when substituting both-end phenalenyl rings of IDPL by donor (NH_2)/acceptor (NO_2) groups. In the latter case, DA-IDPL also exhibits a γ value that is more than 2 orders of magnitude larger than that in the reference closed-shell PY2. In addition, the associated reduction of the diradical character in this open-shell singlet system due to either the application of an electric field or the substitution by donor/acceptor groups is an advantage toward improved thermal stability. The present results therefore provide a new direction to optimize the structure of open-shell singlet systems exhibiting gigantic and tunable third-order NLO responses.

■ ASSOCIATED CONTENT

Supporting Information. Optimized geometries of IDPL and PY2 at $F = 0.0$ and 0.0077 a.u. as well as of DA-IDPL and DA-PY2. Mulliken spin and net charge densities of IDPL and PY2 at $F = 0.0$ and 0.0077 a.u.. Diradical characters, the ground-state dipole moments, and γ_{xxxx} values of IDPL and PY2 under static electric fields ranging from 0.0 to 0.0077 a.u.. This material is available free of charge via the Internet at <http://pubs.acs.org>.

■ AUTHOR INFORMATION

Corresponding Author

*E-mail: mnaka@cheng.es.osaka-u.ac.jp.

■ ACKNOWLEDGMENT

This work was supported by a Grant-in-Aid for Scientific Research (Nos. 21350011 and 20655003) and the “Japan–Belgium Cooperative Program” (J091102006) from the Japan Society for the Promotion of Science (JSPS) and the global COE (center of excellence) program “Global Education and Research Center for Bio-Environmental Chemistry” of Osaka University. Theoretical calculations were partly performed using the Research Center for Computational Science, Okazaki, Japan. L.R. thanks the Fund for Scientific Research – FNRS for her postdoctoral grant within the convention n° 2.4520.11. This work has also been supported by the Academy Louvain (ARC “Extended- π -Conjugated Molecular Tinkertoys for Optoelectronics, and Spintronics”) and by the Belgian Government (IUAP No P06-27 “Functional Supramolecular Systems”).

■ REFERENCES

(1) Novoselov, K. S.; Geim, A. K.; Morozov, S. V.; Jiang, D.; Zhang, Y.; Dubonos, S. V.; Grigorieva, I. V.; Firsob, A. A. Electric Field Effect in Atomically Thin Carbon Films. *Science* **2004**, *306*, 666–669.

(2) Geim, A. K.; Novoselov, K. S. The Rise of Graphene. *Nat. Mater.* **2007**, *6*, 183–191.

(3) Lambert, C. Towards Polycyclic Aromatic Hydrocarbons with a Singlet Open-Shell Ground State. *Angew. Chem., Int. Ed.* **2011**, *50*, 1756–1758.

(4) Du, A.; Smith, S. C. Electronic Functionality in Graphene-Based Nanoarchitectures: Discovery and Design via First-Principles Modeling. *J. Phys. Chem. Lett.* **2011**, *2*, 73–80.

(5) Rieger, R.; Müllen, K. Forever Young: Polycyclic Aromatic Hydrocarbons as Model Cases for Structural and Optical Studies. *J. Phys. Org. Chem.* **2010**, *23*, 315–325.

(6) Terrones, M.; Botello-Mendez-A., R.; Campos-Delgado, J.; Lopez-Urias, F.; Vega-Cantu, Y. I.; Rodriguez-Macias, F. J.; Elias, A. L.; Munoz-Sandoval, E.; Cano-Marquez, A. G.; Charlier, J. C.; Graphene and Graphite Nanoribbons: Morphology, Properties, Synthesis, Defects and Applications. *Nano Today* **2010**, *5*, 351–372.

(7) (a) Bendikov, M.; Duong, H. M.; Starkey, K.; Houk, K. N.; Carter, E. A.; Wudl, F. Oligoacenes. Theoretical Prediction of an Open Shell Singlet Ground State and a Constant, Semiconductor Type HOMO–LUMO Gap. *J. Am. Chem. Soc.* **2004**, *126*, 7416–7417. (b) Erratum: Bendikov, M.; Duong, H. M.; Starkey, K.; Houk, K. N.; Carter, E. A.; Wudl, F. *J. Am. Chem. Soc.* **2004**, *126*, 10493.

(8) Kubo, T.; Shimizu, A.; Uruichi, M.; Yakushi, K.; Nakano, M.; Shiomi, D.; Sato, K.; Takui, T.; Morita, Y.; Nakasuji, K. Singlet Biradical Character of Phenalenyl-Based Kekulé Hydrocarbon with Naphthoquinoid Structure. *Org. Lett.* **2007**, *9*, 81–84.

(9) Shimizu, A.; Uruichi, M.; Yakushi, K.; Matsuzaki, H.; Okamoto, H.; Nakano, M.; Hirao, Y.; Matsumoto, K.; Kurata, H.; Kubo, T. Resonance Balance Shift in Stacks of Delocalized Singlet Biradicals. *Angew. Chem., Int. Ed.* **2009**, *48*, 5482–5486.

(10) Huang, J.; Kertesz, M. Intermolecular Covalent π – π Bonding Interaction Indicated by Bond Distances, Energy Bands, and Magnetism in Biphenalenyl Biradicaloid Molecular Crystal. *J. Am. Chem. Soc.* **2007**, *129*, 1634–1643.

(11) Konishi, A.; Hirao, Y.; Nakano, M.; Shimizu, A.; Botek, E.; Champagne, B.; Shiomi, D.; Sato, K.; Takui, T.; Matsumoto, K.; Kurata, H.; Kubo, T. Synthesis and Characterization of Teranthene: A Singlet Biradical Polycyclic Aromatic Hydrocarbon Having Kekulé Structures. *J. Am. Chem. Soc.* **2010**, *132*, 11021–11023.

(12) Tönshoff, C.; Bettinger, H. F. Photogeneration of Octacene and Nonacene. *Angew. Chem., Int. Ed.* **2010**, *49*, 4125–4128.

(13) Son, Y.; Cohen, M. L.; Louie, S. G. Half-Metallic Graphene Nanoribbons. *Nature* **2006**, *444*, 347–349.

(14) Zheng, H.; Duley, W. Field Effects on the Electronic and Spin Properties of Undoped and Doped Graphene Nanodots. *Phys. Rev. B* **2008**, *78*, 155118.

(15) Yazyev, O. V.; Wang, W. L.; Meng, S.; Kaxiras, E. Comment on Graphene Nanoflakes with Large Spin: Broken-Symmetry States. *Nano Lett.* **2008**, *8*, 766.

(16) Du, A. J.; Zhu, Z. H.; Smith, S. C. Multifunctional Porous Graphene for Nanoelectronics and Hydrogen Storage: New Properties Revealed by First Principle Calculations. *J. Am. Chem. Soc.* **2010**, *132*, 2876–2877.

(17) Schrier, J. Helium Separation Using Porous Graphene Membranes. *J. Phys. Chem. Lett.* **2010**, *1*, 2284–2287.

(18) Hayes, E. F.; Siu, A. K. Q. Electronic Structure of the Open Forms of Three-Membered Rings. *J. Am. Chem. Soc.* **1971**, *93*, 2090–2091.

(19) Yamaguchi, K. In *Self-Consistent Field: Theory and Applications*; Carbo, R.; Klobukowski, M., Eds.; Elsevier: Amsterdam, The Netherlands, 1990; p 727.

(20) Takatsuka, K.; Fueno, T.; Yamaguchi, K. Distribution of Odd Electrons in Ground-State Molecules. *Theor. Chim. Acta* **1978**, *48*, 175–183.

(21) Head-Gordon, M. Characterizing Unpaired Electrons from the One-Particle Density Matrix. *Chem. Phys. Lett.* **2003**, *372*, 508–511.

(22) Nakano, M.; Fukui, H.; Minami, T.; Yoneda, K.; Shigetani, Y.; Kishi, R.; Champagne, B.; Botek, E.; Kubo, T.; Ohta, K.; Kamada, K.

(Hyper)polarizability Density Analysis for Open-Shell Molecular Systems Based on Natural Orbitals and Occupation Numbers. *Theor. Chem. Acc.* **2011**, 10.1007/s00214-010-0871-y.

(23) Kamada, K.; Ohta, K.; Shimizu, A.; Kubo, T.; Kishi, R.; Takahashi, H.; Botek, E.; Champagne, B.; Nakano, M. Singlet Diradical Character from Experiment. *J. Phys. Chem. Lett.* **2010**, 1, 937–940.

(24) Nakano, M.; Kishi, R.; Ohta, S.; Takahashi, H.; Kubo, T.; Kamada, K.; Ohta, K.; Botek, E.; Champagne, B. Relationship between Third-Order Nonlinear Optical Properties and Magnetic Interactions in Open-Shell Systems: A New Paradigm for Nonlinear Optics. *Phys. Rev. Lett.* **2007**, 99, 033001.

(25) Nakano, M.; Kishi, R.; Nitta, T.; Kubo, T.; Nakasuji, K.; Kamada, K.; Ohta, K.; Champagne, B.; Botek, E.; Yamaguchi, K. Second Hyperpolarizability (γ) of Singlet Diradical System: Dependence of γ on the Diradical Character. *J. Phys. Chem. A* **2005**, 109, 885–891.

(26) Nakano, M.; Kishi, R.; Nakagawa, N.; Ohta, S.; Takahashi, H.; Furukawa, S.; Kamada, K.; Ohta, K.; Champagne, B.; Botek, E.; Yamada, S.; Yamaguchi, K. Second Hyperpolarizabilities (γ) of Bisimidazole and Bistriazole Benzenes: Diradical Character, Charged State and Spin State Dependences. *J. Phys. Chem. A* **2006**, 110, 4238–4243.

(27) Ohta, S.; Nakano, M.; Kubo, T.; Kamada, K.; Ohta, K.; Kishi, R.; Nakagawa, N.; Champagne, B.; Botek, E.; Takebe, A.; Umezaki, S.; Nate, M.; Takahashi, H.; Furukawa, S.; Morita, Y.; Nakasuji, K.; Yamaguchi, K. Theoretical Study on the Second Hyperpolarizabilities of Phenalenyl Radical Systems Involving Acetylene and Vinylene Linkers: Diradical Character and Spin Multiplicity Dependences. *J. Phys. Chem. A* **2007**, 111, 3633–3641.

(28) Fukui, H.; Shigeta, Y.; Nakano, M.; Kubo, T.; Kamada, K.; Ohta, K.; Champagne, B.; Botek, E. Enhancement of Second Hyperpolarizabilities in Open-Shell Singlet Slipped-Stack Dimers Composed of Square Planar Nickel Complexes Involving *o*-Semiquinonato Type Ligands. *J. Phys. Chem. A* **2011**, 115, 1117–1124.

(29) Nagai, H.; Nakano, M.; Yoneda, K.; Kishi, R.; Takahashi, H.; Shimizu, A.; Kubo, T.; Kamada, K.; Ohta, K.; Botek, E.; Champagne, B. Signature of Multiradical Character in Second Hyperpolarizabilities of Rectangular Graphene Nanoflakes. *Chem. Phys. Lett.* **2010**, 489, 212–218.

(30) Kamada, K.; Ohta, K.; Kubo, T.; Shimizu, A.; Morita, Y.; Nakasuji, K.; Kishi, R.; Ohta, S.; Furukawa, S.-i.; Takahashi, H.; Strong Two-Photon Absorption of Singlet Diradical Hydrocarbons. *Angew. Chem., Int. Ed.* **2007**, 46, 3544–3546.

(31) Nakano, M.; Champagne, B.; Botek, E.; Ohta, K.; Kamada, K.; Kubo, T. Giant Electric Field Effect on the Second Hyperpolarizability of Symmetric Singlet Diradical Molecules. *J. Chem. Phys.* **2010**, 133, 154302.

(32) Meyers, F.; Marder, S. R.; Pierce, B. M.; Brédas, J. L. Electric Field Modulated Nonlinear Optical Properties of Donor–Acceptor Polyenes: Sum-Over-States Investigation of the Relationship between Molecular Polarizabilities (α , β , and γ) and Bond Length Alternation. *J. Am. Chem. Soc.* **1994**, 116, 10703–10714.

(33) Kirtman, B.; Champagne, B.; Bishop, D. M. Electric Field Simulation of Substituents in Donor-Acceptor Polyenes: A Comparison with Ab Initio Predictions for Dipole Moments, Polarizabilities, and Hyperpolarizabilities. *J. Am. Chem. Soc.* **2000**, 122, 8007–8012.

(34) For IDPL, due to symmetry, there is no field-induced molecular rotation, and the field-free Eckart conditions are satisfied. The situation is different for PY2 because the PY2 has no mirror symmetry with respect to the perpendicular plane involving the axis of the applied pump field, which results in a small component of dipole moment along the *y* axis (0.43 a.u.), together with the dominant component along the *x* axis (5.76 a.u.). See: Luis, J. M.; Duran, M.; Andrés, J. L.; Champagne, B.; Kirtman, B. Finite Field Treatment of Vibrational Polarizabilities and Hyperpolarizabilities: on the Role of the Eckart Conditions, their Implementation, and their Use in Characterizing Key Vibrations. *J. Chem. Phys.* **1999**, 111, 875–884.

(35) Tawada, Y.; Tsuneda, T.; Yanagisawa, S.; Yanai, T.; Hirao, K. A Long-Range-Corrected Time-Dependent Density Functional Theory. *J. Chem. Phys.* **2004**, 120, 8425–8433.

(36) Cohen, H. D.; Roothaan, C. C. J. Electric Dipole Polarizability of Atoms by the Hartree–Fock Method. I. Theory for Closed-Shell Systems. *J. Chem. Phys.* **1965**, 43, S34–S39.

(37) Kishi, R.; Bonness, S.; Yoneda, K.; Takahashi, H.; Nakano, M.; Botek, E.; Champagne, B.; Kubo, T.; Kamada, K.; Ohta, K.; Tsuneda, T. Long-Range Corrected Density Functional Theory Study on Static Second Hyperpolarizabilities of Singlet Diradical Systems. *J. Chem. Phys.* **2010**, 132, 094107.

(38) Nakano, M.; Shigemoto, I.; Yamada, S.; Yamaguchi, K. Size-Consistent Approach and Density Analysis of Hyperpolarizability: Second Hyperpolarizabilities of Polymeric Systems with and without Defects. *J. Chem. Phys.* **1995**, 103, 4175–4191.

(39) Frisch, M. J.; Trucks, G. W.; Schlegel, H. B.; Scuseria, G. E.; Robb, M. A.; Cheeseman, J. R.; Scalapini, G.; Barone, V.; Mennucci, B.; Petersson, G. A.; Gaussian 09, revision A.1; Gaussian, Inc.; Wallingford, CT, 2009.

(40) Bishop, D. M.; Hasan, M.; Kirtman, B. A Simple Method for Determining Approximate Static and Dynamic Vibrational Hyperpolarizabilities. *J. Chem. Phys.* **1995**, 103, 4157–4159.